Eur J Plant Pathol (2011) 130:29–43
DOI 10.1007/s10658-010-9729-3

Metabolomics technology to phenotype resistance in barley against *Gibberella zeae*

G. Kenchappa Kumaraswamy · Venkatesh Bollina · Ajjamada C. Kushalappa · Thin M. Choo · Yves Dion · Sylvie Rioux · Orval Mamer · Denis Faubert

Accepted: 6 December 2010 / Published online: 6 January 2011

Abstract The mechanisms of resistance in barley to fusarium head blight (FHB), caused by *Gibberella zeae* are complex. Metabolomics technology was explored to phenotype resistance. Spikelets of barley genotypes with contrasting levels of resistance to FHB, mock inoculated or with the pathogen, were extracted with aqueous methanol and the metabolites were analyzed using liquid chromatography and hybrid mass spectrometry. Peaks were de-convoluted using XCMS and annotated using CAMERA and IntelliXtract bioinformatics tools. A *t*-test, of a total of 1608 purified peaks, selected 626 metabolites with significant treatment effects, of which 161 were identified as resistance related (RR) metabolites. A total of 53 metabolites, that are RR or pathogenicity related (PR), were assigned with putative compound names. These mainly belonged to three metabolic pathways: fatty acid (jasmonic acid, methyl jasmonate, 9,10- dihydroisojasmonate, linolenic acid, linoleic acid, traumatic acid), phenylpropanoid (*p*-coumaric acid, caffeyl alcohol, dimethoxy-4-phenylcoumarin, rosmarinic acid, diphyllin, 5-methoxypodophyllotoxin) and flavonoid (naringenin, catechin, quercetin, and alpinumisoflavone). A few PR/RR metabolites significantly reduced mycelial growth of *G. zeae* in vitro.

Keywords *Gibberella zeae* · *Fusarium graminearum* · *Hordeum vulgare* · Metabolomics · Mass spectrometry · Barley · Liquid chromatography · Fusarium head blight · Quantitative resistance

G. K. Kumaraswamy · V. Bollina · A. C. Kushalappa (✉)
Plant Science Department, McGill University,
Sainte-Anne-de-Bellevue, QC H9X 3V9, Canada
e-mail: ajjamada.kushalappa@mcgill.ca

T. M. Choo
Eastern Cereal and Oilseed Research Centre,
Agriculture and Agri-Food Canada,
960 Carling Ave.,
Ottawa, ON K1A 0C6, Canada

Y. Dion
Centre de recherche sur les grains inc.,
740 chemin Trudeau,
Saint-Mathieu-de-Beloeil, QC J3G 4S5, Canada

S. Rioux
Centre de recherche sur les grains inc.,
2700 rue Einstein,
Ste. Foy, QC G1P 3W8, Canada

O. Mamer
Goodman Cancer Research Centre, McGill University,
1160 Pine Ave West,
Montréal, QC H3A 1A3, Canada

D. Faubert
Institut de recherches cliniques de Montréal,
110 av. des Pins Ouest,
Montréal, QC H2W 1R7, Canada

Introduction

Fusarium head blight (FHB) or scab of barley, caused by *Gibberella zeae* (anamorph *Fusarium graminearum*), is an important disease affecting several economically important crops belonging to Triticeae including wheat, barley and triticale. FHB not only reduces grain yield but also produces several mycotoxins in grains. Among these, deoxynivalenol (DON) is one of the most common trichothecene toxins (Joffe 1986). Breeding for host resistance is considered to be the most economical and environmentally acceptable disease management method.

Resistance in barley and wheat to FHB is evaluated mainly on two resistance types, even though five types have been proposed (Mesterhazy 1995). Type I is the resistance to infection of spikelets, while type II is resistance to spread of infection within a spike (Schroeder and Christensen 1963). Since cultivated barley genotypes have very high type II resistance, the breeding for resistance has been mainly concentrated on type I resistance (Bushnell et al. 2003; Steffenson 2003). However, these evaluations were mainly conducted under field conditions, and the genotype ranking of resistance was inconsistent over years and locations. Molecular characterization of resistance has led to the identification of more than 100 FHB resistance quantitative trait loci (QTL) in wheat and barley (de la Penna et al. 1999; Mesfin et al. 2003; Buerstmayr et al. 2009). However, less than a third of these QTLs are stable and the function of only the QTL on chromosome 3BS is partially known; the mechanism of resistance is partially associated with detoxification of a fungal virulence factor, DON, to DON-3-*O*-glucoside, by an enzyme UDP-glucosyltransferase (Poppenberger et al. 2003; Lemmens et al. 2005). The occurrence of several FHB resistance QTLs in wheat and barley indicates that several resistance mechanisms are involved and the identification of QTLs or phenotyping resistance based only on symptoms is inadequate.

Metabolomics has been used to phenotype resistance in wheat against *Gibberella zeae* and several pathogenesis related (Hamzehzarghani et al. 2005) and resistance related metabolites have been identified in different genotypes (Hamzehzarghani et al. 2008a; Paranidharan et al. 2008). The pathogenicity related (PR) metabolites are those that are over expressed following pathogen inoculation, while the resistance related (RR) metabolites are those that have higher concentration in a resistant genotype compared to a susceptible genotype. The RR metabolite concentration is inversely related to the fungal biomass in a resistant genotype, so most of these have plant origin. Also, irrespective of variation in genetic background several RR metabolites in wheat against FHB have been identified (Hamzehzarghani et al. 2008a). However, these studies were based on gas chromatography and mass spectrometry (GC/MS) where several of the RR metabolites such as glucosinolates, terpenoids, flavonoids, etc. that are nonvolatile cannot be detected by this method (Vorst et al. 2005). Accordingly, metabolic profiling based on liquid chromatography and mass spectrometry (LC/MS) is essential to phenotype resistance (Schauer and Fernie 2006; Bedair and Sumner 2008). Targeted metabolite analysis has been used to discriminate resistant and susceptible *Brachypodium* sp. against *Magnaporthe grisea* Allwood et al. 2006). In the study presented here, metabolomics technology based on LC coupled to a hybrid mass spectrometer (LC-ESI-LTQ-Orbitrap) was employed to phenotype resistance in two-row barley with cleistogamous florets, against *G. zeae*. Our earlier paper addressed resistance in six-row barley genotypes with chasmogamous florets (Bollina et al. 2010). Under field conditions, the former is more resistant than the latter. The resistance related (RR) metabolites were selected by pair-wise comparison of metabolite abundances between resistant and susceptible cultivars of barley, mock-inoculated and with the pathogen. The functions of these PR/RR metabolites were further explored in a comprehensive bank of plant metabolites with proven defence roles against biotic stress. Furthermore, the antimicrobial properties were demonstrated for a few compounds against *G. zeae*.

Materials and methods

Plant production

Two two-row, yellow barley genotypes H106-4 and H106-371, resistant and susceptible to FHB, respectively, were selected from a population of 190 doubled-haploid lines developed from a cross between Léger and CI9831 (Choo et al. 2004). Two-row barley was selected here because these genotypes have higher

levels of resistance because of cleistogamous florets, unlike six-row barley and most wheat genotypes which have chasmogamous florets, where the spores deposited on lemma and palea have to pass through the resistance barrier before reaching the ovary. Three seeds of each genotype were sown in 15 cm pots, and maintained under green house conditions at 22±3°C. Plants were irrigated daily and fertilized at two-week intervals with 200 ml of 0.3% PlantProd (20-20-20 of NPK + trace elements). Following germination, only the main stem and a tiller for each plant were retained.

Pathogen production, inoculation and incubation

Seven-day old cultures of *Gibberella zeae* (Schwein) Petch (anamorph: *Fusarium graminearum* Schwabe) isolate 15–35 on SNA media (Nirenberg 1981) were flooded with an aqueous solution of 0.02% Tween 80, and filtered through two layers of cheesecloth. The final spore count was adjusted to 1×10^5 macroconidia ml^{-1}. Barley spikelets, at 50% anthesis to early milky stage (GS=65–73; Zadoks et al. 1974), were spray inoculated until run-off using an airbrush (Badger, model: 200.3™, deluxe set) for metabolic profiling and determination of type I resistance. Each treatment was replicated five times. The mock treatment contained aqueous solution of 0.02% Tween 80. The inoculated plants were covered with plastic bags, sprayed inside with sterile water, for 48 h to facilitate initial establishment of infection.

Experimental design

The experiment was conducted as a completely randomized block design with four treatments, two genotypes H106-4 (R = resistant) and H106-371 (S = susceptible) and two inoculations of mock (M=0.02% Tween80) and pathogen (P = macroconidia in 0.02% Tween80), with five replicates conducted over about a week interval. Each experimental unit consisted of a sample of 50–60 spikelets collected from three plants or six spikes from one pot.

Disease severity assessment

The number of diseased spikelets in each spike was recorded at 2 d intervals until the two consecutive readings were the same. From these data the proportion of spikelets diseased out of mid ten spikelets (PSD) on 14 d, and the area under the disease progress curve (AUDPC) (Hamzehzarghani et al. 2005) were determined and used to evaluate type I resistance. The experiment was designed as a completely randomized block, with five blocks over time. The experimental units consisted of 12 spikes for the spray inoculation to assess the type I resistance. Analysis of variance was performed using SAS (version 9.2; SAS Institute Inc., Cary, N. C.).

Sampling and metabolite extraction

For metabolite extraction, 50–60 spray inoculated spikelets from six spikes per treatment, were harvested and frozen immediately with liquid nitrogen and stored at −80°C, for up to a month. The samples were crushed in liquid nitrogen using mortar and pestle. A 100 mg (fresh weight) of finely powdered sample was weighed into a 2.2 ml micro-centrifuge tube to which 400 μl of ice cold methanol (HPLC grade 99.96% pure, Fisher Scientific), 18 μl of genistein (*m/z*=270.0528; 3.7×10^4 pg μl^{-1} of methanol) and 133 μl of water were added to make the final concentration of aqueous methanol to 65%. The samples were sonicated for 15 min at 40 kHz frequency in a water bath and centrifuged for 10 min at 20,000 g at room temperature. The supernatants were filtered through a 0.22 μm PVDF membrane filter (Millipore Corporation, Bedford, USA) and centrifuged at 10,000 rpm for 10 min. The filtrates were collected in glass vials and stored at −20°C and were analyzed the next day.

Metabolite analysis using LC-ESI-LTQ-Orbitrap

Metabolic profiles were developed using a LC hybrid MS system, described in a recently published study by Bollina et al. (2010), with a few modifications. The samples were loaded into a 96 well plate and analyzed using an LC-ESI-LTQ Orbitrap (Thermo Fisher, Waltham, MA). The chromatographic separations were performed using a capillary reverse phase C-18 column (500 μm i.d.×10 cm) packed with 5 μm particle 300 Å Jupiter stationary phase (Phenomenex, Torrance, CA) and maintained at 25°C. Ammonium acetate (2.5 mM, A) and 100% methanol (B) were used as mobile phases. The mass resolution was set at 60,000 at *m/z* 400. Three additional MS/MS events were triggered by the MS scan and acquired in

parallel in the linear ion trap for the top three most intense ions. For MS/MS mode, the normalized collision energy was maintained at 35 eV, activation q and activation time were set at 0.25 and 30 ms, respectively.

LC/MS output analysis

Peak deconvolution and alignment Raw output files were converted to mzData format and were imported into XCMS 1.12.1 (Smith et al. 2006). Data were processed using a signal to noise threshold of 5:1 and band width of 10 s. The chromatograms were deconvoluted and baseline corrected using "*xcmsSet*". The peak alignment was done based on "group" function where the *m/z* and retention time (RT) intervals of 0.01 and 10 s, respectively, were selected. Through the XCMS platform, the CAMERA bioinformatics tool (Tautenhahn et al. 2007) was used to detect peaks with isotopes, neutral losses, adducts and dimers.

Data sieving The output from XCMS was imported into MS-EXCEL and the peaks not consistent among replicates within a treatment were excluded. Multiple peaks, that were associated with adducts, dimers, neutral losses and isotopes were also excluded from further statistical analyses.

Statistical analyses

The data on peak abundance/intensity (of monoisotopic accurate masses retained following sieving) were subjected to student's *t*-test using SAS (version 9.2; SAS Institute Inc., Cary, NC) to select metabolites that had significant treatment effects. The tests of hypotheses included four treatment combinations: RM vs SM, RP vs RM, SP vs SM, RP vs SP, where R = resistant, S = susceptible, M = mock, P = pathogen. The abundances of peaks with significant treatment effects were log transformed and subjected to canonical discriminant analysis (CDA) using CANDISC procedure of SAS (Johnson 1998) to classify the observations based on scatter plot (Hamzehzarghani et al. 2008a).

The peaks with significant treatment effects, based on *t*-test were further classified into pathogenesis related (PR) and resistance related (RR) metabolites (Hamzehzarghani et al. 2008a). A metabolite with significantly higher abundance in the pathogen-inoculated sample than in mock-inoculated sample was considered as a PR metabolite; a PR metabolite in resistant genotype was considered as PRr (PRr = RP>RM) and in susceptible was considered as PRs (PRs = SP>SM). A metabolite with higher abundance in a resistant than in a susceptible genotype was considered as a RR metabolite. A RR metabolite based on mock inoculations was considered as constitutive (RRC = RM>SM) metabolite. A PRr metabolite in a resistant genotype with abundance greater than that in susceptible pathogen inoculated was considered as an RR induced (RRI = RP>RM and RP>SP) metabolite.

Compound identification

Compounds, PR and RR, were identified based on three criteria: a) accurate mass match with databases; b) number of carbons in the molecular formulae based on isotope ratio; and c) confirmation through fragmentation pattern match with databases. Where possible, identities were confirmed by comparisons of retention times and MS/MS spectra with those of authentic compounds. The accurate masses of the metabolites were used to generate possible chemical formulae which were matched with those in METLIN and other public databases (Tohge and Fernie 2009), including KNApSAcK (http://kanaya.naist.jp/KNApSAcK/KNApSAcK-v1200/KNApSAcK.php); MassBank (http://www.massbank.jp/index.html); and McGill-MD (http://metabolomics.mcgill.ca). The median accurate mass error (AME) of the internal standard, genistein, for the 20 samples was −0.35 ppm. The MS/MS fragmentation patterns of the major fragments, when available, were manually confirmed using ChemSketch options of IntelliXtract. The isotopic pattern of $^{12}C/^{13}C$ was used to determine if it contained only the carbon isotopes based on IntelliXtract v. 12 (ACD labs, Toronto). For those that passed this rule the maximum number of possible carbon atoms was calculated, based on the relative abundances of the ^{12}C and ^{13}C peaks using the formula: No. of carbon = (^{13}C isotopic ion abundance/^{12} C ion abundance) * (0.9893/0.0107) (Lijima et al. 2008).

Relative antifungal activity and resistance equivalence of PR/ RR metabolites

The antifungal activities against *G. zeae* in vitro were determined, based on radial fungal colony diameter

reduction, for selected PR/ RR metabolites: methyl jasmonate, *p*-coumaric acid, linolenic acid, linoleic acid, and oleic acid along with ferulic acid as a positive check. A disc-diffusion study was performed in sterile Petri plates of 100 mm in diameter. The RR metabolites were individually added to autoclaved PDA media, to make the final concentrations of 0, 2.5, 5.0 and 7.5 mM, just before the medium curdled. After solidification of media 6 mm discs of seven day old fungus was placed at the center of Petri plates. The plates were incubated at 22°C and the radial growths were measured on the 10th day. The experiment was replicated three times. The colony diameters of each experimental unit were divided by the colony diameter of the control to obtain colony diameter ratios. The colony diameter ratios for three concentrations of each RR metabolite and for each replicate were subjected to the Probit procedure of SAS to derive LD_{50} values (Lethal dose for 50% mycelial inhibition) for each metabolite, which were further subjected to analysis of variance to identify treatments having significant effects, using SAS.

The resistance equivalence (RE) was calculated as: RE = RA/LD_{50}, where RA was the relative abundance of RR metabolites (ratio of abundance in resistant over susceptible) and LD_{50} was the antifungal activity for 50% mycelial inhibition of *G. zeae*.

Results

Disease severity

The barley genotypes H106-4 and H106-371 significantly varied in their resistance to FHB, based on spray inoculation, with PSD=0.25 and 0.45, AUDPC=2.9 and 4.8, respectively, meaning the former had moderate type I resistance, while the latter was susceptible.

Metabolic profiles

A total of 1810 peaks with signal to noise ratio ≥5:1 were detected in this study. Following exclusion of multiple peaks with isotopes, neutral losses, dimers, and adducts, a total 1608 peaks were retained. A *t*-test of the abundances of these 1608 peaks identified 626 significant peaks at $P \leq 0.05$. The abundances of these 626 peaks were subjected to canonical discriminant analysis. The scatter plot grouped each treatment to a separate cluster with minimal error among replicates. The CAN1 vector (explained 65% of variance) discriminated the genotypes explaining constitutive resistance while, the CAN2 vector (explained 28% of variance) discriminated pathogen and mock treatments, and thus, was considered to mainly explain induced resistance (Fig. 1).

PR and RR metabolites

Among 626 significant peaks, 256 were pathogenesis or resistance related, which were designated here as metabolites. Among these, 161 were RR metabolites, including RRC=128 and RRI=33, and 95 were PR metabolites, including PRr=68 and PRs=27. A total of 53 PR or RR metabolites were assigned a tentative identity (Tables 1 and 2). The PR and RR metabolites were:

i) *Pathogenesis related metabolites, in resistant genotype (PRr = RP>RM)*: A total of 68 metabolites were detected as PRr, of which only 17 were tentatively assigned a name (Tables 1 and 2). These included fatty acids: jasmonic acid ($P \leq 0.01$) and its ester methyl jasmonate ($P \leq 0.001$), 2-ethyl-3E-hexenoic acid, linolenic acid, n-heptanoyl acetic acid, tetradecanedioic acid, hydroxy stearic acid, and octadecanedioic acid; phenylpropanoids: *p*-coumaric acid, methyl cinnamate, and diphyllin.

ii) *Pathogenesis related metabolites, in susceptible genotypes (PRs = SP>SM)*: A total of 27 metabolites were detected as PRs metabolites, of which only three were assigned putative names (Tables 1 and 2). These PRs metabolites included few important fatty acids: oleic, pelargonic and heptadecatrienoic acids.

iii) *Resistance related constitutive metabolites (RRC = RM>SM)*: A total of 128 metabolites were detected as RRC, of which 28 were assigned putative names (Tables 1 and 2). These included phenylpropanoid: caffeyl alcohol; flavonoids: naringenin, catechin, 7-hydroxy-5,4′-dimethoxyflavan, 7,8,4′-trihydroxy-3-methoxyflavone, 3,4,5-trihydroxy-3,7-dimethoxyflavone; and terpene: rishitinol and fatty acid: linoleic acid.

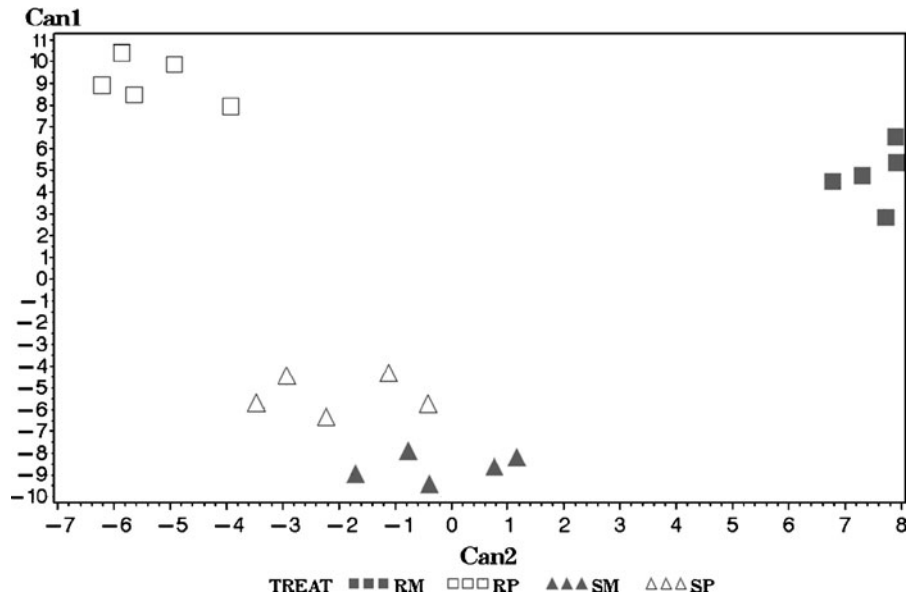

Fig. 1 Scatter plot of treatment significant metabolites using canonical discriminant analysis. RM=resistant mock, RP=resistant pathogen, SM=susceptible mock, SP=susceptible pathogen. The variations explained by canonical vectors are: CAN1=65% (discriminated the genotypes, resistant from susceptible to FHB) and CAN2=28% (discriminated the inoculation types, mock from pathogen inoculated)

iv) *Resistance related induced metabolites (RRI = RP>RM and RP>SP)*: Even though 68 metabolites were detected as PRr, only 33 were detected as RRI, of which only five were assigned putative names (Tables 1 and 2), and these were a phenylpropanoid: rosmarinic acid; flavonoids: quercetin 5,7,3′,4′-tetramethyl ether, and quercetol B; and other: citric acid and aniline.

Relative mycelial inhibition of *G. zeae* and resistance equivalence of PR/RR metabolites

Seven PR/RR metabolites: methyl jasmonate, linoleic acid, linolenic acid, oleic acid, caffeic acid (significant only at $P \leq 0.1$), *p*-coumaric acid and ferulic acid were tested for in vitro mycelial growth inhibition of *G. zeae*. Ferulic acid, though not identified here as an RR metabolite, was used as a positive check since it was reported to have a hyphal inhibitory role against *G. zeae* (Boutigny et al. 2009). Both the types and concentrations of compounds significantly varied in their degree of hyphal inhibition. All six PRr/RR metabolites significantly ($P \leq 0.01$) inhibited the mycelial growth except oleic acid, which is detected as PRs metabolite. Fifty percent inhibition of mycelial growth was found for methyl jasmonate at 1 mM, ferulic acid at 2.4 mM; caffeic acid at 2.5 mM and *p*-coumaric acid at 2.6 mM; linolenic and linoleic acids at 3.6 mM; and oleic acid at 5.6 mM concentrations.

The resistance equivalence for PR/RR metabolites evaluated here varied from zero for ferulic acid (not identified here as RR) to 2.4 for methyl jasmonate (Table 3). A higher RE value indicates a higher level of resistance.

Discussion

The two barley genotypes, with cleistogamous florets, used in this study were doubled-haploid lines, with contrasting levels of resistance to FHB, and were developed from a cross between Léger and CI9831 (Choo et al. 2004). They significantly varied in type I resistance to FHB. The genotype H106-4 was more resistant with significantly lower PSD and AUDPC than the susceptible H106-371. In addition, a field study indicated that the resistant genotype H106-4 had a three year average DON content of 3.3 ppm, while the susceptible H106-371 had 10 ppm (Choo, T. M. Unpublished). For this study the two-row barley genotypes were selected because these have cleistogamous florets, and thus, can better reveal resistance in lemma and palea, avoiding direct inoculation into the ovary during anthesis.

This study reports a total of 128 = RRC, 33 = RRI and 68 = PRr metabolites for FHB in two-row barley. Of these 50 metabolites were tentatively assigned names. The RR metabolites identified here included not only phenolics and fatty acids, as reported earlier based on

Table 1 Resistance related metabolites[a], tentatively identified, from barley spikelets inoculated with mock or *G. zeae*, based on LC-ESI-LTQ-Orbitrap analyses, in negative electrospray ionization

Observed mass (M) median to control)	RT (min) median	Theoretical mass (M)	AME (ppm)	Major fragments MS/MS	RR metabolites Tentative ID[b]	RR/PR metabolites	Abundance (relative	Database[c] Spectral match ()
93.058	8.47	93.0578	−2.7	–	Aniline	RRI	2.4	A;C
103.0635	2.27	103.0633	−1.5	–	Aminobutyric acid	RRC	1.4	A;B;C
119.057	29.8	119.0582	−2.9	**117.97, 99.98, 71.94**	Homoserine	RRC	1.7	A(MID 288);B
119.0583	2.8	119.0582	−1	**73.92, 118.01**	Threonine	RRC*	1.2	A(MID 32); C(KOX00585)
128.0835	39.06	128.0837	1.3	–	Heptenoic acid	RRC **	2.0	A
129.0426	2.44	129.0426	0.03	–	Pyroglutamic acid[b]	PRr*	1.9	A;B
135.0685	8.17	135.0684	−0.86	–	2-Phenylacetamide	PRr	3.4	A
142.0993	36.18	142.0994	0.98	–	2-Ethyl-3E-hexenoic acid	PRr	4.1	A
149.051	2.89	149.0511	0.86	–	Methionine	PRr*	2.7	A;B;C
150.0528	2.29	150.0528	0.29	–	Ribulose	RRC	2.0	A;B
158.1303	38.78	158.1307	2.3	**157.16, 139.08**	Pelargonic acid[b]	PRs	1.3	A;C (KO001673)
162.0683		162.0681	−1.3	**–**	Methyl cinnamate	PRr	2.4	A
164.0473	34.47	164.0473	0.26	**145.25, 119.20, 95.17**	*p*-Coumaric acid	PRr	1.9	A;B;C (KO000445); D (McGill MD)
166.0629	31.63	166.063	0.67	–	Caffeyl alcohol	RRC**	2.2	A;B
168.1149	34.96	168.115	0.39	–	2Z,4E-decadienoic acid	RRC*	2.8	A
172.1097	40.89	172.1099	1.4	–	n-Heptanoyl acetic acid	PRr	2.6	A
192.0277	2.46	192.027	−3.6	**111.14, 173.12,** 149.0	Citric acid	RRI *	2.1	A(MID 124); B;C (MT000044)
196.058	2.3	196.0583	1.5	–	Gluconic acid	RRC	2.1	A;B;C
196.1461	40.99	196.1463	1.2	–	Dodecadienoic acid	RRC	2.3	A
200.1046	40.1	200.1048	1	–	Dioxo-decanoic acid	RRC*	2.5	A
200.1772	43.22	200.1776	1.9	–	Lauric acid	RRC*	1.4	A;B;C
204.0896	2.73	204.0899	1.4	–	Tryptophan	RRC*	2.3	A;B;C
210.1254	26.25	210.1256	−0.95	**191.02, 165.04, 163.14**	Jasmonic acid	PRr*	2.6	A;B;D(McGill MD)
214.1929	42.04	214.1933	1.7	–	10-Methyl lauric acid	RRC	1.5	A
224.1411	34.95	224.1412	0.54	**223.02, 205.11, 195.27, 179.21**	Methyl jasmonate[b]	PRr**	2.4	A;B;D(McGill MD)
224.1773	39.26	224.1776	1.4	223.08, 205.18, 179.13	Tetradecynoic acid	RRC*	2.0	A

Table 1 (continued)

Observed mass (M) median to control)	RT (min) median	Theoretical mass (M)	AME (ppm)	Major fragments MS/MS	RR metabolites Tentative ID[b]	RR/PR metabolites	Abundance (relative	Database[c] Spectral match ()
226.1565	37.67	226.1569	1.8	–	(+)-9,10-Dihydro-7-isojasmonic acid	PRr*	2.3	A;B
228.136	28.26	228.1361	0.42	209.08, 199.13, 165.1	Traumatic acid	RRC*	1.2	A
228.2084	42.03	228.2089	2	–	Myristic Acid[b]	RRC*	1.4	A;B;C
234.1616	39.01	234.1619	1.3	233.18	Rishitinol[b]	RRC	2.1	B
258.1825	37.76	258.1831	2.2	225.15, 193.13	Tetradecanedioic acid	PRr*	5.7	A
264.2083	41.82	264.2089	2.1	–	Heptadecatrienoic acid	PRs	8.5	A
272.068	29.54	272.0685	1.9	**151.07, 177.05, 165.09**	Naringenin	RRC	2.0	A;B;D(McGill MD)
274.1774	33.28	274.178	2.2	241.15, 209.23, 191.12, 165.26	3-Hydroxytetradecanedioic acid[b]	RRC	1.6	A
274.1915	31.69	274.1933	−0.96	121, 119, 106.96, 104.98	Apo-13-zeaxanthinone	RRC	1.2	A
278.2242	40.6	278.2246	1.2	**233.22, 179.11**	Linolenic acid[b]	PRr*	2.8	A;B;C (MT000072); D (McGill MD)
280.2397	42.1	280.2402	1.7	**279.19, 261.23,**	Linoleic acid[b]	RRC	1.6	A(MID 191);B;C (MT000114); D(McGill MD)
282.0891	2.29	282.0964	0.36	–	Dimethoxy-4-phenylcoumarin	RRC	2.9	A;B
282.2553	41.29	282.2559	2.1	**281.31, 263.22**	Oleic acid[b]	PRs*	2.1	A(MID 190);B;C (MT000029); D(McGill MD)
284.2343	41.97	284.2351	2.6	239.32, 211.07, 152.87	2-Methoxy-6Z-hexadecenoic acid[b]	RRC	2.1	A
290.0784	11.38	290.079	2	**245.08, 205.06, 203.04**	Catechin	RRC*	1.3	A(MID 3419);B
290.1876	36.99	290.1882	2.19	–	Deoxy phytoprostane J1	RRC	2.4	B
300.0628	31.69	300.0633	1.7	**284.03;** 271.0; **227.04**	3,5,7′-Trihydroxy-4-methoxyflavone[b]	RRC*	1.3	A;B; C(PR040031)
300.2658	43.1	300.2664	1.9	231.02, 197.34,183.1	Hydroxy stearic acid[b]	PRr*	3.0	A
314.245	40.05	314.2457	2.1	295.22, 183.13	Octadecanedioic acid[b]	PRr*	2.3	A
330.0732	32.45	330.0852	2.4	241.02, 229.32, 223.1	5,7,2′-Trihydroxy-8,6′-dimethoxyflavone	RRC*	3.2	B
358.1072	2.28	358.1053	−3.5	–	Quercetin 5,7,3′,4′-tetramethyl ether	RRI	1.9	A;B

360.0836	31.93	360.0845	2.4	–	Rosmarinic acid	RRI *	1.9	A;B;C
364.1269	42.73	364.1311	−3.7	–	Alpinumisoflavone dimethyl ether	PRr	6.1	B
368.2	41.13	368.1987	−3.4	–	Quercetol B	RRI *	1.1	A;B
380.0891	2.32	380.0807	1.2	217.16, 179.05	Diphyllin[b]	PRr	3.1	B
390.1669	34.79	390.1598	2.4	241.06, 169.49, 155.01	5-Methoxy-trans-dihydrodehydrodiconiferyl alcohol	PRr	1.7	B
444.141	31.58	444.142	2.3	235.12, 207.09, 193	5-Methoxypodophyllotoxin	PRr	2.1	B

Acronyms, abbreviations and symbols: Median *m/z*: Detected in the LC/MS output based on XCMS analysis; AME (ppm): The accurate mass error in ppm ((Observed – Exact)/Exact). Metabolites with no asterisk: $P \leq 0.05$ significance, *: $P \leq 0.01$ significance, **: $P \leq 0.001$ significance; Major fragments: only the most intense fragments were listed; and the bold font indicates a match in database/s; PRr: pathogenesis related resistant, RRC: resistance related constitutive, RRI: resistance related induced, PRs: pathogenesis related susceptible metabolites

[a] Out of 626 treatment significant metabolites 161 = RR metabolites and 95 PR metabolites; only the RR and PR metabolites that were tentatively identified (AME ≤5 ppm) with a name are presented

[b] These are the names of RR metabolites that passed the isotope ratio $^{12}C/^{13}C$ criteria according to IntelliXtract v.12 and also had satisfied the maximum numbers of carbon match criteria

[c] Database: A=METLIN; B=KNApSAcK; C=MassBank; D=McGill MD. In parenthesis, respective compound labels of MS/MS spectra are presented

GC/MS analyses (Hamzehzarghani et al. 2008a, b; Paranidharan et al. 2008), but also flavonoids and terpenoids, similar to those reported by Bollina et al. (2010). A signal molecule, jasmonic acid (JA) identified here as PRr metabolite, is known to play an important role in plant resistance against stress (Farmer 2007; Balbi and Devoto 2008). Methyl jasmonate had the lowest LD_{50} value for inhibition of mycelial growth of *G. zeae* and also had the highest resistance equivalence, among the seven PR/RR metabolites tested here. However, this metabolite was not detected as a RR metabolite by Bollina et al. (2010). This study further confirms our earlier study (Bollina et al. 2010) on the application of metabolomics technology, based on LC-ESI-LTQ-Orbitrap analyses, for phenotyping resistance through identification of resistance related metabolites and resistance equivalence for metabolites in plants against biotic stress. The significant progress made in comprehensive metabolomics of the barley-*Gibberella* interaction system and its application to phenotype resistance in plants against biotic stress is important.

Metabolite analysis based on LC-ESI-LTQ-Orbitrap and peak annotation

We found the high resolution, high mass accuracy and dynamic range for ion detection characteristics of the LC-ESI-LTQ-Orbitrap a great advantage in this study. The instrument operates in MS mode (1 spectrum s^{-1}) with nominal mass resolving power of 60,000 and provides high-accuracy mass measurements of <2 ppm (Makarov et al. 2006). Several fine tuning steps were needed to improve the performance of this instrument. A change in the sheath gas from 8 to 20 along with the

Table 2 Metabolites with significant treatment effects[a] detected from barley-*G. zeae* interaction system

Treatment combination	Metabolites	Tentatively identified
PRr = RP>RM	68	17
PRs = Sp>SM	27	3
RRC = RM>SM	128	28
RRI = RP>SP ; RP>RM	33	5
Total (RR and PR)	256	53

[a] The significant treatment effect was based on RM>SM, RP>RM, SP>SM and RP>SP, where R=resistant, S=susceptible, M=mock, P=pathogen inoculated

Table 3 Resistance equivalence[a] for resistance related metabolites in barley genotype H106-4, considering H106-371 as susceptible

RR metabolites	Relative abundance	LD_{50} Con. (mM)	Resistance equivalence
Caffeic acid	2.2	2.5	0.88
p-coumaric acid	1.9	2.6	0.73
Ferulic acid	0[b]	2.4	0
Linoleic acid	1.6	3.6	0.44
Linolenic acid	2.8	3.6	0.78
Methyl jasmonate	2.4	1.0	2.4
Oleic acid	2.1	5.6	0.35

[a] Resistance equivalence (RE) for metabolites = relative abundance/LD_{50} concentration in mM; where the relative abundance of metabolite = abundance in resistant genotype/abundance in susceptible. Greater RE values indicate higher levels of resistance in the resistant genotype relative to susceptible

[b] Ferulic acid was not identified here as RR metabolite, thus it was given here a zero value

resolution from 30,000 to 60,000 increased the detection of peaks from 800 to close to 2000 per run. Furthermore, high chromatographic resolution is crucial in metabolomics to avoid coelution which can lead to errors in identification of metabolites.

Peak annotation in LC-MS based metabolomics is one of the greatest challenges (Moco et al. 2007; de Vos et al. 2007). Metabolite identification using LC-MS was achieved through a combination of accurate masses, fragmentation patterns and isotopic distribution (Table 1) (Moco et al. 2007). We achieved AME $\leq$2 ppm for most of the compounds detected which reduced the number of possible choices in searching databases (Kind and Fiehn 2007). Fragmentation pattern of parent ions was used to assign structures and the fragmentation pattern was manually verified using the IntelliXtract bioinformatics tool (IntelliXtract v. 12, ACD labs, Canada). In addition, isotopic patterns were used to estimate the number of carbon atoms present and minimize the number of alternative chemical formulae (Table 1) (Kind and Fiehn 2007; Lijima et al. 2008). Several of the metabolites were tentatively identified by matching accurate masses and fragmentation patterns with those in KNApSAcK, METLIN and MassBank and a few from KEGG and HMDB. As the number of authentic plant secondary metabolites commercially available is small and many are impure and/or unstable, the use of these standards is considered not a feasible method for large scale compound identification (Matsuda et al. 2009). In spite of this a few RR metabolites were bought, spiked and the spectra were matched with those observed (Table 1). Thus, the fragmentation patterns reported here for other metabolites should be considered quite reliable. Among the 256 RR/PR metabolites reported here, only 53 were tentatively identified. However, the RR metabolites or accurate masses not assigned with names here are still valid fingerprints of resistant barley phenotypes and they can be identified in future, and related to metabolic pathways to better explain resistance.

Comparative metabolomics systems and factors influencing resistance

Resistance in Triticeae against FHB is controlled by several mechanisms, and not all mechanisms can be explained based on metabolomics. The plant defence roles of hundreds of metabolites have been individually proven (Vidhyasekaran 2008) but often in polygenic resistance several of these act together, and the literature on such a role is lacking. Thus our goal here was to apply metabolomics to phenotype resistance. Accordingly, we chose a barley genotype expected to have several mechanisms of resistance against *G. zeae* (Hamzehzarghani et al. 2008b; Bollina et al. 2010). Most plant defences in plants are based on metabolites and proteins (Agrios 2005; Vidhyasekaran 2008). Since metabolites are the end products of 'omics', they can better represent the phenotype, providing information on response to perturbation in biological systems (Fiehn et al. 2007; Sumner et al. 2003). The metabolites are cell, tissue and organ specific, and accordingly in our study only the spikelets, rather than the entire spike

(Lemmens et al. 2005; Hamzehzarghani et al. 2008a), were used. Organ specific gene expression within a spikelet has been reported, where the caryopsis had different gene expression from that of lemma and palea; while the latter two had similar profiles (Golkari et al. 2007). The spikelets sampled in our study contained mainly lemma and palea, with minimal caryopsis. A compound can occur as more than one peak in a scan event, representing adducts isotopes and neutral losses upon LC/MS analyses. These different forms of a compound were detected here using CAMERA. Statistical analyses of these metabolites, with no sieving steps, can lead to erroneous conclusions (Evans et al. 2009). In addition, unlike multivariate analysis, the identification of resistance related metabolites based on a *t*-test can reveal constitutive and induced metabolites.

Metabolic pathways and roles of RR metabolites

The RR metabolites tentatively identified in our study were linked to their metabolic pathways to better explain their role in plant defence. In addition to RR metabolites the PRr metabolites were also explored for their role in resistance. Most of the PRr and RR metabolites or their precursors belonged to four major metabolic pathways that are known to produce several secondary metabolites with antimicrobial, signalling and cell wall enforcement properties. Several transcriptomics and proteomics studies also have implied possible production of many of the PRr and RR metabolites reported here (Geddes et al. 2008; Li and Yen 2008).

i) *Phenylpropanoid metabolism*: In this study, seven phenylpropanoid RR metabolites were tentatively assigned names. We detected caffeyl alcohol, a precursor of lignin, and dimethoxy-4-phenylcoumarin as RRC, and rosmarinic acid as RRI. In addition, *p*-coumaric acid was detected as a PRr metabolite. Several phenylpropanoids identified here as RR metabolites were also reported in barley (Bollina et al. 2010) and wheat against *G. zeae* (Hamzehzarghani et al. 2008a; Paranidharan et al. 2008; Siranidou et al. 2002), further confirming the occurrence of common RR metabolites against FHB across genera and genotypes. *p*-Coumaric acid showed 50% mycelial inhibition of *G. zeae* in vitro at 2.6 mM concentration (Table 3) and was also inhibitory to both *F. graminearum* and *F. culmorum* in vitro (McKeehen et al. 1999; Bollina et al. 2010). Phenylpropanoids are known for their antioxidant properties. Boutigny et al. (2009) have demonstrated inhibition of all trichothecene synthesis by *G. zeae* following application of ferulic acids to cultures and the mode of action was considered to be due to the antioxidant properties of these metabolites. Thus, several of the RR metabolites, phenolics and flavonoids, reported here should also be able to inhibit the production of trichothecene toxins. Ferulic acid also reduced fungal development (Boutigny et al. 2009; Siranidou et al. 2002; Bollina et al. 2010), and we report here other phenylpropanoids with relative mycelial inhibition greater than that by ferulic acid, which had LD_{50}=2.4 mM concentration.

Polymerization of phenolic compounds to form lignins and lignans is also a common mode of defence in several plants (Naoumkina et al. 2010). In our study we detected two lignans called diphyllin and 5-methoxypodophyllotoxin as PRr metabolites. Cho et al. (2007) isolated three lignans from nutmeg and found them to be antifungal in vitro.

ii) *Flavonoid metabolism*: A total of eight flavonoids were assigned with putative names such as, naringenin, catechin, quercetin, and alpinumisoflavone. Naringenin and catechin were identified as RRC metabolites. Naringenin was found to inhibit rice blast fungus in vitro (Mizutani et al. 1996). Catechin was the most common flavonoid present in barley and was found induced in resistant naked barley seeds after artificial inoculation of *F. graminearum* (Eggert et al. 2010). They also postulated that catechin may represent a valuable marker to explain high resistance in barley to *Fusarium* spp. as compared to wheat. In our study we detected catechin in lemma and palea, contrasting to their detection in naked seeds. The flavonoids are synthesized in metabolic pathways downstream from phenylpropanoids. We have not detected salicylic acid as an RR metabolite, and questioning its role in resistance in barley against *G. zeae*. Instead we observed production of several phenylpropanoids leading to the production of several phenolics, precursors of lignin, and lignans.

Similar to phenylpropanoids, the flavonoids also can act as antioxidents and are capable of inhibiting trichothecene synthesis (Boutigny et al. 2009). It was reported that a methyltransferase (naringenin 7-*O*-methyltransferase (NOMT)) catalyzing the methylation of naringenin (5,7,4′-trihydroxyflavanone) to sakuranetin was induced by JA (Tamogami et al. 1997). In our study we detected both naringenin and JA as RR metabolites against FHB. Both of these greatly reduced mycelial growth of *G. zeae* in vitro.

iii) *Fatty acid metabolism*: A total of 17 fatty acids with significant treatment effects were tentatively identified. JA ($P \leq 0.01$) and methyl jasmonate ($P \leq 0.001$) were identified here as PR metabolites in resistant (PRr) but not in susceptible (PRs) genotype, where traumatic acid accumulated as an RRC metabolite (Table 1; Fig. 2). Methyl jasmonate had the lowest LD_{50} value (1 mM) and the highest resistance equivalence (Table 3). JA is an important signalling molecule for plant defence and stress responses (Farmer 2007; Balbi and Devoto 2008). Methyl jasmonate is a well known plant stress hormone which causes activation of programmed cell death and other defence mechanisms in vivo (Zhang and Xing 2008). In addition we report here that it also has antifungal properties. Membrane-bound phospholipase can release linolenic acid which is then oxidized to JA under stress. In wheat cultivar Sumai3, allene oxide synthase, a key enzyme in JA biosynthesis was up-regulated against *G. zeae* inoculation, along with lipoxygenase enzyme, which clearly indicated the induction of the JA signalling pathway as a resistance mechanism (Li and Yen 2008). The *Arabidopsis* mutants lacking JA production genes were extremely susceptible to *Pythium mastophorum* that causes root rot, and an exogenous application reduced the disease incidence (Vijayan et al. 1998). Transgenic rice overexpressing a JA-biosynthetic gene had enhanced resistance to the pathogenic fungus *M. grisea*,

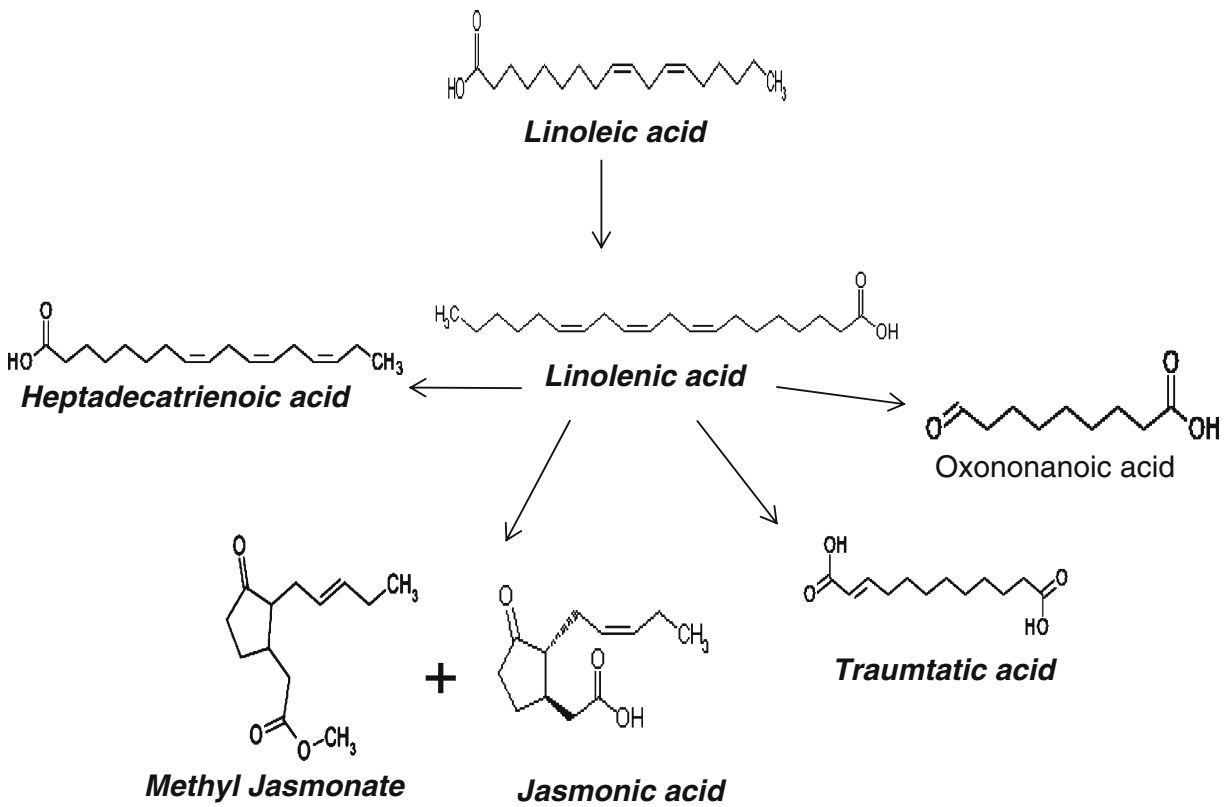

Fig. 2 Part of the fatty acid metabolic pathway showing induction of linolenic and other related acids, following inoculation of barley spikelets with *G. zeae*, leading to the production of signalling molecules jasmonic acid and methyl jasmonate

which causes blast disease (Mei et al. 2006). JA is induced against necrotrophic pathogens (*Botrytis cinerea*) in *Arabidopsis* (Glazebrook 2005). *G. zeae* is a necrotrophic pathogen, and higher abundance of JA in resistant genotype further proves the role of JA in plant and necrotrophic pathogen interaction. Dihydro-7-iso-jasmonic acid, another derivative of JA was also tentatively identified as a PRr metabolite ($P \leq 0.01$). We postulate that the JA signalling pathway is the major resistance mechanism in barley against *G. zeae*.

Linolenic, oleic and linoleic acids, precursors for JA biosynthesis (Fig. 2), were also identified as PRr and RR metabolites in wheat against FHB (Hamzehzarghani et al. 2008a). Both linolenic and linoleic acids exhibited in vitro inhibition of several pathogenic fungi: *Rhizoctonia solani*, *Pythium ultimum*, *Pyrenophora avenae* and *Crinipellis perniciosa* (Walters et al. 2004). Both linolenic and linoleic acids had a lower LD_{50} value of 3.6 mM as compared to oleic acid which required 5.6 mM concentration for mycelial inhibition (Table 3). The oleic acid is detected here as PRs metabolite, which is further supported here in the antimicrobial study by its inability to inhibit hyphal growth of *F. graminearum*. Both linolenic and linoleic acids are substrates for the production of a range of trihydroxy oxylipins in plants (Hamberg 1999), which have exhibited antifungal activities against *M. grisea* in rice plants (Kato et al. 1985). Traumatic acid, another fatty acid, tentatively identified here as RRC, reduced the hyphal growth of *M. grisea,* in vitro (Yara et al. 2008). The fatty acids not only act as antimicrobials, but also are constitutively deposited to form wax layers and lipids that reduce pathogen penetration and further progress in plants.

Future applications of metabolomics to better understand mechanisms and phenotype resistance

We have demonstrated here the significance of mass spectrometry based metabolomics technology for phenotyping resistance in barley against *G. zeae*. Further improvements in extraction, column technology, etc. are needed to detect other metabolites involved in resistance. The complex polymers, such as lignin and other structural components, considered to be involved in resistance, cannot be detected based on metabolomics, but they can be broken down to simpler forms and identified using GC/MS (Robinson and Mansfield 2009). We have proven the antimicrobial property of metabolites in vitro but proving these in vivo and also other mechanisms such as induced resistance by signal molecules are quite challenging. The RR metabolites identified here can be used as biomarkers to evaluate resistance, following further validation in other genotypes. The PRr metabolites can also be considered as potential biomarkers, as they are found to have antifungal activity as reported in this study. We have also identified several RR accurate masses that were not assigned a name. These accurate masses can be used as biomarkers in breeding, following validation of their occurrence in several resistant genotypes. Hopefully, these unknowns can eventually be identified and related to metabolic pathways in the future with progress in metabolomics technology.

Acknowledgements This project was funded by the Ministère de l'Agriculture, des Pêcheries et de l'Alimentation du Québec (MAPAQ), Centre de recherche sur les grains inc. (CEROM), and the Fédération des producteurs de porc du Québec (FPPQ), Québec, Canada.

References

Agrios, G. N. (2005). *Plant Pathology*. London: Elsevier Academic.

Allwood, J. W., Ellis, D. I., Hield, J. K., Goodacre, R., & Mur, L. A. J. (2006). Metabolomic approaches reveal that phosphatidic and phosphatidyl glycerol phospholipids are major discriminatory non-polar metabolites in responses by *Brachypodium distachyon* to challenge by *Magnaporthe grisea*. *The Plant Journal, 46*, 351–368.

Balbi, V., & Devoto, A. (2008). Jasmonate signaling network in *Arabidopsis thaliana*: crucial regulatory nodes and new physiological scenarios. *New Phytologist, 177*, 301–318.

Bedair, M., & Sumner, L. W. (2008). Current and emerging mass spectrometry technologies for metabolomics. *Trends in Analytical Chemistry, 27*, 238–250.

Bollina, V., Kumaraswamy, G. K., Kushalappa, A. C., Choo, T. M., Dion, Y., Rioux, S., et al. (2010). Mass spectrometry-based metabolomics application to identify quantitative resistance-related metabolites in barley against *Fusarium* head blight. *Molecular Plant Pathology, 11*(6), 769–782.

Boutigny, A. L., Barreau, C., Atanasova-penichon, V., Verdal-bonnin, M., Pinson-gadais, L., & Richard-forget, F. (2009). Ferulic acid, an efficient inhibitor of type B trichothecene biosynthesis and Tri gene expression in Fusarium liquid cultures. *Mycological Research, 113*, 746–753.

Buerstmayr, H., Ban, T., & Anderson, J. A. (2009). QTL mapping and marker-assisted selection for Fusarium head blight resistance in wheat: a review. *Plant Breeding, 128*, 1–26.

Bushnell, W. M. R., Hazen, B. E., & Pritsch, C. (2003). Histology and physiology of Fusarium head blight. In K. J. Leonard & W. R. Bushnell (Eds.), *Fusarium head blight in wheat and barley* (pp. 44–83). St Paul: American Phytopathological Society.

Cho, J. Y., Choi, J. G., Son, W. S., Jang, K. S., Lim, H. K., Lee, S. O., et al. (2007). Isolation and antifungal activity of lignans from *Myristica fragrans* against various plant pathogenic fungi. *Pest Management Science, 63*, 935–940.

Choo, T. M., Vigier, B., Shen, Q. Q., Martin, R. A., Ho, K. M., & Savard, M. (2004). Barley traits associated with resistance to Fusarium head blight and deoxynivalenol accumulation. *Phytopathology, 94*, 1145–1150.

de la Penna, R. C., Smith, K. P., Cappettini, F., Muehlbauer, G. J., Gallo-Meagher, M., Dill-Macky, R., et al. (1999). Quantitative trait loci associated with resistance to Fusarium head blight and kernel discoloration in barley. *Theoretical and Applied Genetics, 99*, 561–569.

de Vos, R. C. H., Moco, S., Lommen, A., Keurentjes, J. J. B., Bino, R. J., & Hall, R. D. (2007). Untargeted large-scale plant metabolomics using liquid chromatography coupled to mass spectrometry. *Nature Protocols, 2*, 778–791.

Eggert, K., Hollmann, J., Hiller, B., Kruse, H. P., Rawel, H. M., & Pawelzik, E. (2010). Effects of Fusarium infection on the phenolics in emmer and naked barley. *Journal of Agricultural Food Chemistry, 58*, 3043–3049.

Evans, A. M., DeHaven, C. D., Barrett, T., Mitchell, M., & Milgram, E. (2009). Integrated, nontargeted ultrahigh performance liquid chromatography/electrospray ionization tandem mass spectrometry platform for the identification and relative quantification of the small molecule complement of biological systems. *Analytical Chemistry, 81*, 6656–6667.

Farmer, E. E. (2007). Jasmonate perception machines. *Nature, 448*, 659–660.

Fiehn, O., Sumner, L. W., Ward, J., Dickerson, J., Lange, M. B., Lane, G., et al. (2007). Minimum reporting standards for plant biology context in metabolomics studies. *Metabolomics, 3*, 195–201.

Geddes, J., Eudes, F., Laroche, A., & Selinger, L. B. (2008). Differential expression of proteins in response to the interaction between the pathogen *Fusarium graminearum* and its host, *Hordeum vulgare*. *Proteomics, 8*, 545–554.

Glazebrook, J. (2005). Contrasting mechanisms of defense against biotrophic and necrotrophic pathogens. *Annual Review of Phytopathology, 43*, 205–227.

Golkari, S., Gilbert, J., Prasher, S., & Procunier, J. D. (2007). Microarray analysis of *Fusarium graminearum*-induced wheat genes: identification of organ specific and differentially expressed genes. *Plant Biotechnology Journal, 5*, 38–49.

Hamberg, M. (1999). An epoxy alcohol synthase pathway in higher plants: biosynthesis of antifungal trihydroxy oxylipins in leaves of potato. *Lipids, 34*, 1131–1142.

Hamzehzarghani, H., Kushalappa, A. C., Dion, Y., Rioux, S., Comeau, A., Yaylayan, V., et al. (2005). Metabolic profiling and factor analysis to discriminate quantitative resistance in wheat cultivars against fusarium head blight. *Physiology and Molecular Plant Pathology, 66*, 119–133.

Hamzehzarghani, H., Paranidharan, V., Abu-Nada, Y., Kushalappa, A., Dion, Y., Rioux, S., et al. (2008a). Metabolic profiling coupled with statistical analyses for potential high throughput screening of quantitative resistance to fusarium head blight in wheat cultivars. *Canadian Journal of Plant Pathology, 30*, 24–36.

Hamzehzarghani, H., Paranidharan, V., Abu-Nada, Y., Kushalappa, A. C., Mamer, O., & Somers, D. (2008b). Metabolic profiling to discriminate wheat near isogenic lines, with quantitative trait loci at chromosome 2DL, varying in resistance against fusarium head blight. *Canadian Journal of Plant Science, 88*, 789–797.

Joffe, A. (1986). In A. Joffe (Ed.), *Fusarium species: Their biology and toxicology* (pp. 225–292). New York: Wiley.

Johnson, D. E. (1998). *Applied multivariate methods for data analysts*. North Scituate, MA: Duxbury Press.

Kato, T., Yamaguchi, Y., Abe, N., Uyehara, T., Namai, T., Kodama, M., et al. (1985). Structures and synthesis of unsaturated trihydroxy C18 fatty acids in rice plant suffering from rice blast disease. *Tetrahedron Letters, 26*, 2357–2360.

Kind, T., & Fiehn, O. (2007). Seven golden rules for heuristic filtering of molecular formulas obtained by accurate mass spectrometry. *BMC Bioinformatics, 8*, 105.

Lemmens, M., Scholz, U., Berthiller, F., Dall'Asta, C., Koutnik, A., Schuhmacher, R., et al. (2005). The ability to detoxify the mycotoxin deoxynivalenol colocalizes with a major quantitative trait locus for fusarium head blight resistance in wheat. *Molecular Plant-Microbe Interactions, 18*, 1318–1324.

Li, G., & Yen, Y. (2008). Jasmonate and ethylene signaling pathway may mediate Fusarium head blight resistance in wheat. *Crop Science, 48*, 888–896.

Lijima, Y., Nakamura, Y., Ogata, Y., Tanaka, K., Sakurai, N., Suda, K., et al. (2008). Metabolite annotations based on the integration of mass spectral information. *The Plant Journal, 54*, 949–962.

Makarov, A., Denisov, E., Kholomeev, A., Balschun, W., Lange, O., Strupat, K., et al. (2006). Performance evaluation of a hybrid linear ion trap/orbitrap mass spectrometer. *Analytical Chemistry, 78*, 2113–2120.

Matsuda, F., Yonekura-Sakakibara, K., Niida, R., Kuromori, T., Shinozaki, K., & Saito, K. (2009). MS/MS spectral tag-based annotation of non-targeted profile of plant secondary metabolites. *The Plant Journal, 57*, 555–577.

McKeehen, J. D., Busch, R. H., & Fulcher, R. G. (1999). Evaluation of wheat (*Triticum aestivum* L.) phenolic acids during grain development and their contribution to *Fusarium* resistance. *Journal of Agricultural Food Chemistry, 47*, 1476–1482.

Mei, C., Qi, M., Sheng, G., & Yang, Y. (2006). Inducible overexpression of a rice allene oxide synthase gene increases the endogenous JA level, PR gene expression, and host resistance to fungal infection. *Molecular Plant Microbe Interaction, 19*, 113–127.

Mesfin, K. P., Smith, K. P., Dill-Macky, R., Evans, C., Waugh, R., Gustus, C., et al. (2003). Quantitative traits loci for Fusarium head blight resistance in barley detected in a two-rowed by six rowed population. *Crop Science, 43*, 307–318.

Mesterhazy, A. (1995). Types and components of resistance to Fusarium head blight in wheat. *Plant Breeding, 114*, 377–386.

Mizutani, A., Miki, N., Yukioka, H., Tamura, H., & Masuko, M. (1996). A possible mechanism of control of rice blast

disease by a novel alkoxyiminoacetamide fungicide, SSF126. *Phytopathology, 86*, 295–300.

Moco, S., Bino, R., de Vos, R. C. H., & Vervoort, J. (2007). Metabolomics technologies and metabolite identification. *Trends in Analytical Chemistry, 26*, 855–866.

Naoumkina, M. A., Zhao, Q., Gallego-giraldo, L., Dai, X., Zhao, P. X., & Dixon, R. A. (2010). Genome-wide analysis of phenylpropanoid defence pathways. *Molecular Plant Pathology, 11*(6), 829–846.

Nirenberg, H. (1981). A simplified method for identifying *Fusarium* spp. occurring on wheat. *Canadian Journal of Botany, 59*, 1599–1609.

Paranidharan, V., Abu-Nada, Y., Hamzehzarghani, H., Kushalappa, A. C., Mamer, O., Dion, Y., et al. (2008). Resistance related metabolites in wheat against *Fusarium graminearum* and virulence factor, DON. *Botany, 86*, 1168–1179.

Poppenberger, F., Berthiller, D., Lucyshyn, T., Sieberer, T., Schuhmacher, R., Krska, R., et al. (2003). Detoxification of the Fusarium mycotoxin deoxynivalenol by a UDP-glucosyltransferase from *Arabidopsis thaliana*. *Journal of Biological Chemistry, 278*, 47905–47914.

Robinson, A., & Mansfield, S. (2009). Rapid analysis of poplar lignin monomer composition by a streamlined thioacidolysis procedure and NIR-based prediction modeling. *The Plant Journal, 58*, 706–714.

Schauer, N., & Fernie, A. R. (2006). Plant metabolomics: towards biological function and mechanism. *Trends in Plant Science, 11*, 508–516.

Schroeder, H. W., & Christensen, J. J. (1963). Factors affecting resistance of wheat to scab by *Gibberella zeae*. *Phytopathology, 53*, 831–838.

Siranidou, E., Kang, Z., & Buchenauer, H. (2002). Studies on symptom development, phenolic compounds and morphological defense responses in wheat cultivars differing in resistance to Fusarium head blight. *Journal of Phytopathology, 150*, 200–208.

Smith, A. C., Elizabeth, J. W., Grace, O., Ruben, A., & Gary, S. (2006). XCMS: Processing mass spectrometry data for metabolite profiling using nonlinear peak alignment, matching, and identification. *Analytical Chemistry, 78*, 779–787.

Steffenson, B. J. (2003). Fusarium head blight of barley: Impact, epidemics, management, and strategies for identifying and utilizing genetic resistance. In K. J. Leonard & W. R. Bushnell (Eds.), *Fusarium head blight of wheat and barley* (pp. 241–295). St. Paul: APS.

Sumner, W. L., Mendes, P., & Richard, A. D. (2003). Plant metabolomics: large-scale phytochemistry in the functional genomics era. *Phytochemistry, 62*, 817–836.

Tamogami, S., Rakwal, R., & Kodama, O. (1997). Phytoalexin production by amino acid conjugates of JA through induction of naringenin 7-*O*-methyltransferase, a key enzyme on phytoalexin biosynthesis in rice (*Oryza sativa* L.). *FEBS Letters, 401*, 239–242.

Tautenhahn, R., Böttcher, C., & Neumann, S. (2007). Annotation of LC/ESI-MS mass signals. Proceedings of BIRD 2007 - *1st International Conference on Bioinformatics Research and Development*, Springer LNBI 4414.

Tohge, T., & Fernie, A. R. (2009). Web-based resources for mass-spectrometry-based metabolomics: A user's guide. *Phytochemistry, 70*, 450–456.

Vidhyasekaran, P. (2008). *Fungal pathogenesis in plants and crops*. Boca Raton: CRC.

Vijayan, P., Shockey, J., Lévesque, C. A., Cook, R. J., & Browse, J. (1998). A role for jasmonate in pathogen defense of *Arabidopsis*. *PNAS, 95*, 7209–7214.

Vorst, O., de Vos, C. H. R., Lommen, A., Staps, R. V., Visser, R. G. F., Bino, R. J., et al. (2005). A non-directed approach to the differential analysis of multiple LC-MS derived metabolic profiles. *Metabolomics, 1*, 169–180.

Walters, D., Raynor, L., Mitchell, A., Walker, R., & Walker, K. (2004). Antifungal activities of four fatty acids against plant pathogenic fungi. *Mycopathologia, 157*, 87–90.

Yara, A., Yaeno, T., Montillet, J. L., Hasegawa, M., Seo, S., Kusumi, K., et al. (2008). Enhancement of disease resistance to *Magnaporthe grisea* in rice by accumulation of hydroxylinoleic acid. *Biochemical and Biophysical Research Communications, 370*, 344–347.

Zadoks, J. C., Chang, T. T., & Konzak, B. F. (1974). A decimal code for the growth stages of cereals. *Weed Research, 14*, 415–421.

Zhang, L., & Xing, D. (2008). Methyl jasmonate induces production of reactive oxygen species and alterations in mitochondrial dynamics that precede photosynthetic dysfunction and subsequent cell death. *Plant Cell Physiology, 49*, 1092–1111.